ACS Medicinal Chemistry Letters

pubs.acs.org/acsmedchemlett Letter

Discovery of Dipeptides as Potent Botulinum Neurotoxin A Light-Chain Inhibitors

Martin Amezcua, Ricardo S. Cruz, Alex Ku, Wilfred Moran, Marcos E. Ortega, and Nicholas T. Salzameda*

Cite This: *ACS Med. Chem. Lett.* 2021, 12, 295−301 Read Online

ACCESS | Metrics & More | Article Recommendations | Supporting Information

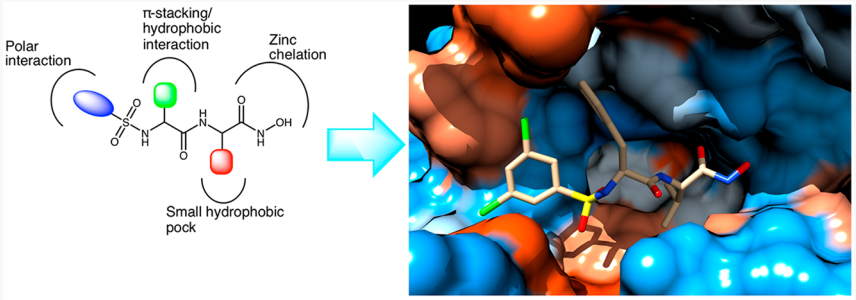

33 (PDB# 7KYH)
IC_{50} = 21 nM for the BoNT/A light chain

ABSTRACT: The botulinum neurotoxin, the caustic agent that causes botulism, is the most lethal toxin known to man. The neurotoxin composed of a heavy chain (HC) and a light chain (LC) enters neurons and cleaves SNARE proteins, leading to flaccid paralysis, which, in severe occurrences, can result in death. A therapeutic target for botulinum neurotoxin (BoNT) intoxication is the LC, a zinc metalloprotease that directly cleaves SNARE proteins. Herein we report dipeptides containing an aromatic connected to the N-terminus via a sulfonamide and a hydroxamic acid at the C-terminus as BoNT/A LC inhibitors. On the basis of a structure−activity relationship study, **33** was discovered to inhibit the BoNT/A LC with an IC_{50} of 21 nM. X-ray crystallography analysis of **30** and **33** revealed that the dipeptides inhibit through a competitive mechanism and identified several key intermolecular interactions.

KEYWORDS: *Dipeptide, botulinum neurotoxin, protease inhibitor, hydroxamic acid*

The botulinum neurotoxin (BoNT) is a metabolic byproduct of the *Clostridium botulinum* bacteria and causes the paralytic disease botulism. In humans, botulism is commonly caused by the consumption of improperly processed foods (i.e., meats and canned food) contaminated with the BoNT or by the consumption of the bacteria, which grows in the intestinal tract and releases the toxin.[1,2] There are seven serotypes of the toxin categorized A−G, with BoNT/A being the most toxic, with an LD_{50} of 1.3 ng/kg in humans, making it the most lethal toxin known to man.[3,4] It is estimated that ∼1 g of BoNT/A can kill 1 million people.[5,6] This has elevated BoNT as a potential bioterrorism weapon[7,8] due to the high toxicity and ease of producing the toxin. BoNT has several clinical applications to treat neuromuscular and neuronal diseases;[1] however, overexposure can lead to intoxication, even when using controlled clinical doses. The current countermeasures available for BoNT intoxication are antitoxins, but they have many drawbacks, such as a limited treatment window (>48 h post exposure)[9] once infected. In addition, the dangerous side effects[9] and the high cost of producing the antitoxins highlight their issues and demonstrate that they would not be an ideal treatment during a widespread biological attack.[7,8] Therefore, new therapeutics, specifically small molecules that are more cost effective and can enter cells to increase the treatment window, are urgently needed to counter the deadly effects of a potential large-scale BoNT outbreak.

The neurotoxin is composed of a 100 kDa heavy chain (HC) and 50 kDa light chain (LC) linked by a single disulfide bond.[1,10,11] The HC is composed of two active domains, a translocation domain at the N-terminus and a binding domain at the C-terminus.[1] The binding domain recognizes neurons by binding to a ganglioside and a protein receptor.[1,11] The translocation domain inserts the LC, a Zn^{2+}-dependent metalloprotease, into the cytosol of neurons and is a critical

Received: December 22, 2020
Accepted: January 25, 2021
Published: January 27, 2021

https://dx.doi.org/10.1021/acsmedchemlett.0c00674
ACS Med. Chem. Lett. 2021, 12, 295−301

Scheme 1. Synthesis of Dipeptides[a]

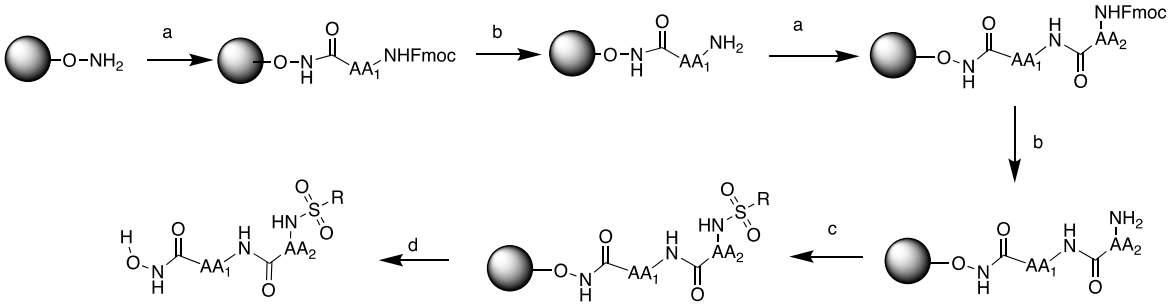

[a]Reagents and conditions: (a) Fmoc-protected amino acid, HOBt, DIC, DMF; (b) 25% PIP in DMF; (c) sulfonyl chloride, 2,6-lutidine, DCM; (d) 50% TFA in DCM.

step for intoxication.[12] Upon internalization into the neuron cytosol, BoNT/A LC cleaves the synaptosome-associated protein (SNAP-25).[1] SNAP-25, vesicle-associated membrane protein (VAMP), and syntaxin make up the SNARE protein complex that is required for docking of synaptic vesicles to the nerve terminal for the controlled release of acetylcholine into the neuromuscular junction for normal neuromuscular and autonomic functions.[12] The cleavage of a single SNARE protein by the BoNT inhibits the formation of the SNARE complex and halts the release of acetylcholine, leading to flaccid muscle paralysis.[1,10,11,13] Severe cases of intoxication lead to cardiac and respiratory failure and eventually death.

Small-molecule therapeutics are advantageous for the treatment of BoNT intoxication on a large scale and would provide relief for BoNT intoxication even after the neurotoxin has entered the cell.[14,15] A promising small-molecule therapeutic target for BoNT/A intoxication is the LC.[14,16,17] A variety of molecules have been reported to bind and inhibit the proteolytic activity of the LC.[15,18]

Our laboratory previously discovered a novel molecular scaffold for BoNT/A LC inhibition,[19] with our best inhibitor having an IC_{50} value of 0.54 μM against the BoNT/A LC.[20] In the present study we have expanded on our amino scaffold by incorporating a second amino acid. The dipeptide includes a hydroxamic acid at the C-terminus, two amino acids with hydrophobic side chains, and a sulfonamide at the N-terminus connecting an aromatic. Reported peptide BoNT/A LC inhibitors are composed of polar amino acid sequences, such as arginine, to interact with zinc and other polar residues in the active site.[21−24] The dipeptides in this work include a hydroxamic acid at the C-terminus to chelate with zinc. The hydroxamic acid is a known metal chelator[25] and a common chemical warhead for BoNT/A LC inhibitors.[14,18,26,27] The hydroxamic acid and N-terminus sulfonamide in our dipeptides will provide the polar contacts. We propose that the hydrophobic amino acid side chains are better suited for BoNT/A LC inhibitors, as they can maximize the interactions with the large hydrophobic active site.[24,27] In addition, the aromatic group attached to the sulfonamide will be available for pi-stacking and additional hydrophobic interactions.

Dipeptides have the potential to be developed into therapeutic treatments. There are several current drugs that contain a dipeptide scaffold, such as enalapril, lisinopril, and spriapril, which are angiotensin-converting enzyme (ACE) inhibitors. The pharmacokinetics of dipeptides are better than those of larger peptides due to intestinal cellular transporters that are specific for di- and tripeptides and have been shown to be responsible for the absorption of several dipeptide drugs.[28−30] Furthermore, dipeptides have been shown to cross the blood−brain barrier,[31] which would be advantageous for botulism therapeutics. Dipeptides are an untapped source of BoNT/A LC inhibitors; therefore, our goal of this current work is to evaluate dipeptides as inhibitors.

Dipeptides were synthesized on hydroxylamine Wang resin using Fmoc-protected amino acids and following standard coupling and deprotection strategies. The dipeptide was deprotected, and the N-terminus reacted with various sulfonyl chlorides under basic conditions to give the completed dipeptide on resin. The resin was treated with acid to release the dipeptide from the resin and reveal the hydroxamic acid (Scheme 1). The crude product was purified by prep-HPLC and freeze-dried to give pure dipeptides (**1**−**33**), as confirmed by analytical HPLC. Compounds **30**−**33** were further confirmed by NMR and HRMS. The dipeptides were studied via a commercial FRET-based BoNT/A LC enzymatic assay (List Laboratories, CA) to determine the percent inhibition or IC_{50} values. Additionally, two crystal structures of the BoNT/A LC bound to dipeptides (**30** and **33**) were solved and analyzed to determine specific intermolecular interactions between the dipeptide and the BoNT/A LC.

A dipeptide amino acid profile study was performed to determine the optimal amino acid sequence for binding and inhibition. We focused on amino acids with nonpolar side chains because the BoNT/A LC active site is large and predominantly hydrophobic[24,32] and thus focused on optimizing the nonpolar binding interactions. Both the hydroxamic acid and sulfonamide were constant throughout this entire study.

The amino acid profile study (Table 1) indicated that the isoleucine at AA_1 is the preferred C-terminal amino acid. As Ile was replaced with a smaller amino acid, Ala (**5**), β-Ala (**15**), or Gly (**16**) inhibition decreased. The substitution of Ile for a larger side chain such as Phe (**6**) also decreased the inhibition. These results are consistent with a small hydrophobic pocket in proximity to the catalytic zinc ion. The *sec*-butyl of Ile fits well in this pocket, as smaller side chains could have fewer interactions, leading to decreased binding. The larger side chain of Phe would not fit in this small pocket and would thereby sterically disrupt zinc chelation and significantly limit binding and inhibition, which was observed for **6**. The incorporation of Aib into the dipeptide also decreased binding. This is most likely due to Aib altering the conformation of the dipeptide, as Aib is known to have drastic effects on the secondary structure of peptides.[33] This result is consistent with

https://dx.doi.org/10.1021/acsmedchemlett.0c00674
ACS Med. Chem. Lett. 2021, 12, 295−301

Table 1. Dipeptide Amino Acid Sequence Study

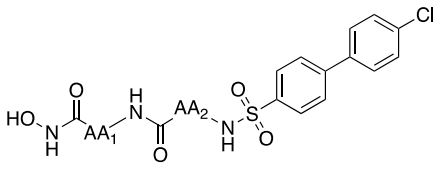

compd.	AA_1	AA_2	% inhibition[a]
1	Ile	Leu	100
2	Ile	Phe	100
3	Ile	Ile	85
4	Ile	Aib	84
5	Ala	Ile	55
6	Phe	Ile	44
7	Ile	Ala	31
8	Aib	Ile	11
9	Ile*	Ile*	48
10	Ile*	Ile	57
11	Ile	Ile*	69
12	Ile*	Phe*	63
13	Phe	Ile*	62
14	Ile	Phe*	41
15	*β*-Ala	Ile	62
16	Gly	Ile	18

[a]Dipeptides were evaluated at 15 μM with 20 nM BoNT/A LC and 8 μM SNAPtide substrate. Enzyme reactions were performed in triplicate, and the percent inhibition reported is the average. *D-amino acid.

our previous study that revealed Ile to be the optimal amino acid at the C-terminus.[20]

Amino acids with large side chains can be accommodated at AA_2, as this position is farther away from the zinc chelation event (Table 1). The AA_2 position is less sensitive to amino acid substitution, as Aib (**4**) resulted in moderate inhibition. In addition, the hydrophobic side chains of AA_2 are in an ideal position to interact with the large hydrophobic cavity. Phe is well suited at AA_2 because the group can participate in π-stacking or other hydrophobic interactions, which is confirmed by the strong inhibition observed for **2**. Leu and Ile at AA_2 (**1** and **3**, respectively) also displayed strong inhibition, as the branched side chains can form more hydrophobic contacts than Ala (**7**), which showed poor inhibition. This result was expected because AA_2 is farther away from zinc binding and in an excellent position to interact with the hydrophobic wall of the active site; therefore, aromatic and branched alkyl side chains would reinforce binding.

The stereochemistry of the amino acids was also evaluated for inhibition (Table 1). As expected, dipeptides containing L-amino acids resulted in better inhibition than D-amino acid dipeptides. This result is not surprising because native amino acids would interact better with the peptide backbone of the active site. It is worth noting that **13** had slightly better inhibition than the L-dipeptide counterpart (**6**). The combination of L-Phe and D-Ile (AA_1 and AA_2, respectively) could result in an alternate binding mode for **13**, leading to the improved inhibition. In our previous amino acid scaffold, we discovered that D-isoleucine was essential for strong inhibition, as the D-amino acid was thought to position the sulfonamide biphenyl into a favorable binding site.[20] Overall, dipeptides containing L-amino acids provided the best inhibition, and this stereochemistry was maintained throughout the study.

The initial dipeptide contained a biphenyl with a chlorine at C-4′, modeled after our previous lead structure.[19,20] We hypothesize that at least one phenyl ring and polar substituent(s) would be essential for inhibition. As observed in other inhibitor studies,[24,32] there are few polar contacts, and these opportunities should be utilized for tight binding to the predominately hydrophobic BoNT/A LC active site. We varied both the phenyl and polar substituents to identify intermolecular interactions (Table 2). Chlorine has been shown to be

Table 2. Probing the Aromatic System on the Dipeptide N-Terminus

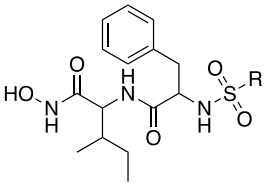

compd.	R	% inhibition[a]
17	biphenyl	77
18	4-cyclohexylphenyl	57
19	phenyl	52
20	3,5-dichlorophenyl	100
21	*meta-tert*-butylphenyl	93
22	*para*-bromophenyl	87
23	*para*-chlorophenyl	77
24	*meta*-chlorophenyl	79
25	3,4-diethoxyphenyl	22
26	2,6-dichlorophenyl	83

[a]Dipeptides were evaluated at 15 μM with 20 nM BoNT/A LC and 8 μM SNAPtide substrate. Enzyme reactions were performed in triplicate, and the percent inhibition reported is the average.

involved in key interactions, specifically with Arg363,[27,32,34] and as expected, without chlorine on the biphenyl, the inhibition decreased. Furthermore, substitution of the biphenyl for 4-cyclohexylphenyl (**18**) or phenyl (**19**) resulted in decreased inhibition, as the cyclohexyl most likely contributed to steric clashes and diminished hydrophobic interactions in regards to **18**. Interestingly, when a halide was added to the phenyl (**22** or **23**), inhibition increased. This supports a key polar interaction that is essential for binding.

The position or type of halide on the phenyl was not crucial for inhibition, as a halide at the para (**23**) or meta (**24**) position did not greatly alter the inhibition. However, the addition of a second chlorine to the phenyl (**20**) drastically improved inhibition, indicating strong polar intermolecular interactions. Another explanation for the strong inhibition of **20** is the electron-withdrawing ability of the chlorines, which would increase the phenyl's π-stacking interactions, leading to tight binding. The position of the chlorines affected the inhibition, as the 2,6-dichlorophenyl analog (**26**) had lower inhibition compared with **20**, indicating that chlorine is involved in a favorable interaction in the meta position, or the ortho position is causing a steric repulsion. This evidence points to the chlorines involved in specific interactions within the active site rather than an electron effect that is strengthening the π-stacking. The addition of ethoxy groups (**25**) also caused the inhibition to significantly decrease. This could be due to a steric effect or the electron-donating nature of the ethoxy groups disrupting the π-stacking. The strong

https://dx.doi.org/10.1021/acsmedchemlett.0c00674
ACS Med. Chem. Lett. 2021, 12, 295−301

inhibition observed for **21** was surprising because this dipeptide does not follow a clear trend with the other dipeptides in this study. The BoNT/A LC has been reported to bind large hydrophobic groups such as adamantane through an induced fit model.[34] The BoNT/A LC active site is known to be highly flexible[32] and could accommodate the hydrophobic *tert*-butyl group of **21** via an induced fit. On the basis of the results of this study, the 3,5-dichrolophenyl contributed to potent inhibition and will be included in second-generation dipeptides.

Second-generation dipeptides were synthesized based on the previous results, and their IC_{50} values for the BoNT/A LC were determined (Table 3). The library focused on branched side chains at both AA_1 and AA_2 in addition to Phe at AA_2. The AA_1 position is more sensitive to branched side chains, as this amino acid is adjacent to the hydroxamic acid. Substituting Ile (**20**) with Val (**33**) resulted in a 7.5-fold decrease in the IC_{50} value. The removal of a methyl group drastically changed the IC_{50} value, indicating a well-defined small hydrophobic pocket in close proximity to the catalytic zinc. The isopropyl of valine fits better in the pocket than the *sec*-butyl of Ile, which demonstrates the sensitivity of the AA_1 position. Poor binding in this pocket disrupts zinc chelation, causing decreased inhibition. This trend is consistent with **32**, as the propyl side chain of Nva would be too long for the pocket, resulting in a two times higher IC_{50} compared with **33**. The second-generation library confirmed our pervious results that a small hydrophobic pocket is in close proximity to the catalytic zinc.

Table 3. Second-Generation Dipeptides

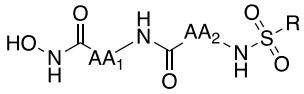

compd.	AA_1	AA_2	R	IC_{50} (μM)[a]
27	Nva	Ile	biphenyl-4-chloro	1.0
2	Ile	Phe	biphenyl-4-chloro	2.4
28	Ile	Val	biphenyl-4-chloro	2.9
20	Ile	Phe	3,5-dichlorophenyl	0.15
29	Leu	Ile	3,5-dichlorophenyl	0.15
30	Nva	Ile	3,5-dichlorophenyl	0.089
31	Ile	Val	3,5-dichlorophenyl	0.069
32	Nva	Phe	3,5-dichlorophenyl	0.043
33	Val	Phe	3,5-dichlorophenyl	0.021

[a]Dipeptides were evaluated using 20 nM BoNT/A LC, 8 μM SNAPtide substrate, and a range of dipeptide concentrations to determine IC_{50} values.

As previously indicated, the AA_2 position is less sensitive to amino acid substitutions and has the potential for numerous hydrophobic interactions. The optimal amino acid at the AA_2 position is Phe, with a potent IC_{50} value of 21 nM for **33**. The phenyl side chain is most likely participating in π-stacking. As expected, the sulfonamide biphenyl analogs (**2**, **27**, and **28**) resulted in modest IC_{50} values ranging from 1 to 3 μM. Replacing the biphenyl with 3,5-dicholorphenyl drastically improved the IC_{50} values to <1 μM. The results confirm that the biphenyl is too large for the dipeptide scaffold. Also, the chlorines on the phenyl are vital for inhibition due to the formation of polar contacts or by effecting the electronics of the phenyl, leading to improved binding.

We solved the crystal structure of the apo BoNT/A LC (PDB 7KY2) and the cocrystal structures of the BoNT/A LC bound to **30** (PDB 7KYF) and **33** (PDB 7KYH) to gain structural insight into dipeptide binding (Table S1 and Figures 1 and 2). Compounds **30** and **33** both displayed the predicted hydroxamate chelation to the active-site zinc. This evidence signifies that the dipeptide scaffolds in this study participate in a competitive mode of inhibition, as observed with other hydroxamate-based inhibitors.[14] In addition, the 3,5-dicholorophenyl sulfonamide of both compounds occupies a similar area between Phe369 and Val70 in the crystal structure. There is no apparent π-stacking observed in this area of the crystal structure for both compounds. The chlorines are involved in polar interactions with the peptide backbone, establishing the chlorines as a key element for binding. Halogen bonding has

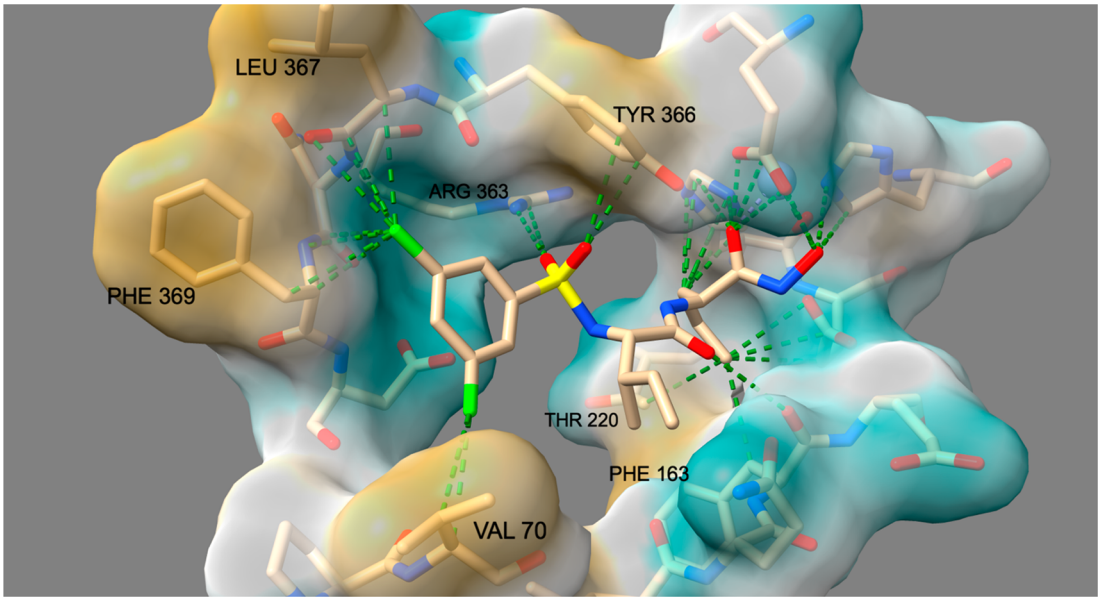

Figure 1. X-ray crystal structure of **30** bound to the BoNT/A LC active site (PDB 7KYF). Green dashed lines represent intermolecular contacts generated with ChimeraX.[36]

https://dx.doi.org/10.1021/acsmedchemlett.0c00674
ACS Med. Chem. Lett. 2021, 12, 295−301

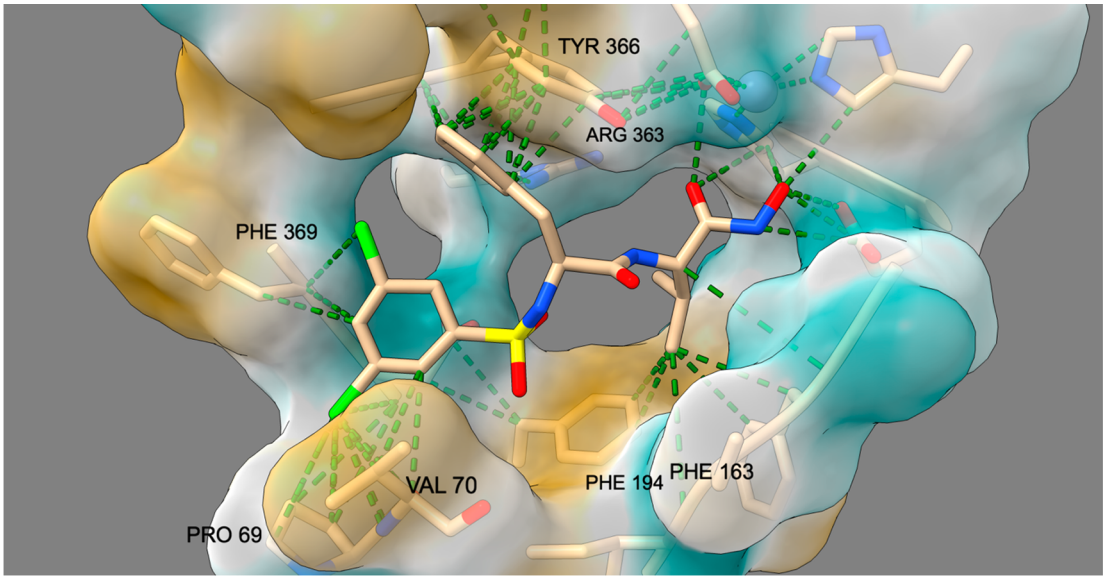

Figure 2. X-ray crystal structure of **33** bound to the BoNT/A LC active site (PDB 7KYH). Green dashed lines represent intermolecular contacts generated with ChimeraX.[36]

been observed in many protein ligand complexes, indicating the importance of this interaction in drug discovery.[35] Overall, the dipeptides occupy the same region within the BoNT/A LC active site. The sulfonamide of **30** participates in contacts with Arg363 and Tyr366 (Figure 1). In our previous molecular modeling study, we proposed that the sulfonamide interacts with Arg363 and acts as the hinge to guide the molecule into the binding sites.[20] The crystal structure validates this theory and also demonstrates the potential for Tyr366 to be involved in this interaction. The polar interaction anchors the molecule in the active site and orientates the Ile side chain toward the opening of the active site. The propyl side chain of Nva is positioned into the previously discovered small hydrophobic pocket formed by Thr220 and Glu224 and adjacent to the catalytic zinc.

In the crystal structures, the side chains of **33** occupy different regions in the BoNT/A LC active site (Figure 2) compared with **30**. The phenyl of Phe is π-stacking with Tyr366, which blocks Arg363 from interacting with the sulfonamide or any other elements of the molecule. The π-stacking is a key interaction for this dipeptide, leading to the low IC_{50} value. The sulfonamide is pointing into the active site but is not involved in any interactions within the active site. The valine side chain is in the small hydrophobic pocket formed by Phe163, Phe194, and Thr220.

Dipeptides with hydrophobic side chains have been shown to be potent inhibitors for the BoNT/A LC. Through a structure−activity relationship study of the dipeptide sequence and sulfonamide aromatic, dipeptide **33** was synthesized and had an IC_{50} of 21 nM. A crystal structure of this dipeptide bound to the BoNT/A LC revealed the hydroxamic acid chelating to the zinc, supporting a competitive mode of inhibition. The side chains of **33** are involved in numerous hydrophobic interactions within the active site, including π-stacking. A well-defined small hydrophobic pocket adjacent to the catalytic zinc was also discovered in this study. In addition, the crystal structure of **30** displays polar interactions between the chlorines and the peptide backbone and between the sulfonamide and Arg363. The inhibition data along with the crystal structures provide a foundation for the future development of dipeptides as potent inhibitors for the BoNT/A LC. These novel BoNT/A LC inhibitors have enormous potential for future optimization as the dipeptide core is amenable to rapid structural changes to improve inhibition. Furthermore, future studies will evaluate the physiochemical properties and investigate the dipeptides in cellular and *in vivo* experiments.

■ ASSOCIATED CONTENT

Supporting Information

The Supporting Information is available free of charge at https://pubs.acs.org/doi/10.1021/acsmedchemlett.0c00674.

Synthesis procedures, analytical data, and details of the enzyme assay, enzyme purification, crystallization, and structure solution (PDF)

■ AUTHOR INFORMATION

Corresponding Author

Nicholas T. Salzameda − *Department of Chemistry & Biochemistry, California State University, Fullerton, California 92831, United States;* orcid.org/0000-0001-5498-4955; Phone: 657-278-3594; Email: nsalzameda@fullerton.edu

Authors

Martin Amezcua − *Department of Chemistry & Biochemistry, California State University, Fullerton, California 92831, United States*

Ricardo S. Cruz − *Department of Chemistry & Biochemistry, California State University, Fullerton, California 92831, United States*

Alex Ku − *Department of Chemistry & Biochemistry, California State University, Fullerton, California 92831, United States*

Wilfred Moran − *Department of Chemistry & Biochemistry, California State University, Fullerton, California 92831, United States*

Marcos E. Ortega − *Department of Chemistry & Biochemistry, California State University, Fullerton,*

https://dx.doi.org/10.1021/acsmedchemlett.0c00674
ACS Med. Chem. Lett. 2021, 12, 295−301

California 92831, United States; orcid.org/0000-0003-3515-9321

Complete contact information is available at: https://pubs.acs.org/10.1021/acsmedchemlett.0c00674

Author Contributions

M.A., R.S.C., and A.K. synthesized dipeptides. M.A. performed inhibitor assays. W.M. expressed and purified BoNT/A LC. M.E.O. grew crystals and solved crystal structures. N.T.S. designed experiments, supervised the dipeptide synthesis and inhibitor assay, and wrote the manuscript. All authors contributed to writing the manuscript and have given approval to the final version of the manuscript.

Notes

The authors declare no competing financial interest.

■ ACKNOWLEDGMENTS

We are grateful to the Allergan Foundation and California State University, Fullerton for financial support of this research. Instrumentation support was provided by the Department of Defense (68816-RT-REP) and the National Science Foundation MRI (CHE1726903) for the acquisition of a UPLC-HRMS apparatus. The X-ray diffraction instrument purchase was supported by the Department of Defense (DoD) Research and Education Program for Historically Black Colleges and Universities and Minority-Serving Institutions (HBCU/MI) Equipment/Instrumentation Grant to S. Chantal E. Stieber under contract no. W911NF-17-1-0537. We also thank the ALS-ENABLE beamlines for collection of X-ray diffraction data. The ALS-ENABLE beamlines are supported in part by the National Institutes of Health, National Institute of General Medical Sciences, grant P30 GM124169-01. The Advanced Light Source is a Department of Energy Office of Science User Facility under contract no. DE-AC02-05CH11231. Molecular graphics and analyses were performed with UCSF ChimeraX, developed by the Resource for Biocomputing, Visualization, and Informatics at the University of California, San Francisco, with support from the National Institutes of Health R01-GM129325 and the Office of Cyber Infrastructure and Computational Biology, National Institute of Allergy and Infectious Diseases.

■ ABBREVIATIONS

BoNT, botulinum neurotoxin; CDC, Centers for Disease Control and Prevention; HC, heavy chain; LC, light chain; SNAP-25, synaptosome-associated protein; VAMP, vesicle-associated membrane protein; ACE, angiotensin-converting enzyme; FRET, fluorescence resonance energy transfer; Fmoc, fluorenylmethoxycarbonyl; HOBt, hydroxybenzotriazole; DIC, *N,N′*-diisopropylcarbodiimide; DMF, *N,N*-dimethylformamide; PIP, piperidine; DCM, dichloromethane; TFA, trifluoroacetic acid; Nva, norvaline; Aib, 2-aminoisobutyric acid

■ REFERENCES

(1) Pirazzini, M.; Rossetto, O.; Eleopra, R.; Montecucco, C. Botulinum Neurotoxins: Biology, Pharmacology, and Toxicology. *Pharmacol. Rev.* **2017**, *69* (2), 200−235.
(2) Simpson, L. The life history of a botulinum toxin molecule. *Toxicon* **2013**, *68*, 40−59.
(3) Gill, D. M. Bacterial toxins: a table of lethal amounts. *Microbiol. Rev.* **1982**, *46* (1), 86−94.
(4) Rossetto, O.; Montecucco, C. Tables of Toxicity of Botulinum and Tetanus Neurotoxins. *Toxins* **2019**, *11* (12), 686.
(5) Arnon, S. S.; Schechter, R.; Inglesby, T. V.; et al. Botulinum toxin as a biological weapon: Medical and public health management. *JAMA* **2001**, *285* (8), 1059−1070.
(6) Bossi, P.; Garin, D.; Guihot, A.; Gay, F.; Crance, J. M.; Debord, T.; Autran, B.; Bricaire, F. Bioterrorism: management of major biological agents. *Cell. Mol. Life Sci.* **2006**, *63* (19−20), 2196−212.
(7) Cenciarelli, O.; Riley, P. W.; Baka, A. Biosecurity Threat Posed by Botulinum Toxin. *Toxins* **2019**, *11* (12), 681.
(8) Janik, E.; Ceremuga, M.; Saluk-Bijak, J.; Bijak, M. Biological Toxins as the Potential Tools for Bioterrorism. *Int. J. Mol. Sci.* **2019**, *20* (5), 1181.
(9) Richardson, J. S.; Parrera, G. S.; Astacio, H.; Sahota, H.; Anderson, D. M.; Hall, C.; Babinchak, T. Safety and Clinical Outcomes of an Equine-derived Heptavalent Botulinum Antitoxin Treatment for Confirmed or Suspected Botulism in the United States. *Clin. Infect. Dis.* **2020**, *70* (9), 1950−1957.
(10) Koussoulakos, S. Botulinum neurotoxin: the ugly duckling. *Eur. Neurol.* **2009**, *61* (6), 331−42.
(11) Dong, M.; Masuyer, G.; Stenmark, P. Botulinum and Tetanus Neurotoxins. *Annu. Rev. Biochem.* **2019**, *88*, 811−837.
(12) Coffield, J. A. Botulinum neurotoxin: the neuromuscular junction revisited. *Crit. Rev. Neurobiol.* **2003**, *15* (3−4), 175−96.
(13) Shukla, H. D.; Sharma, S. K. Clostridium botulinum: a bug with beauty and weapon. *Crit. Rev. Microbiol.* **2005**, *31* (1), 11−8.
(14) Lin, L.; Olson, M. E.; Eubanks, L. M.; Janda, K. D. Strategies to Counteract Botulinum Neurotoxin A: Nature's Deadliest Biomolecule. *Acc. Chem. Res.* **2019**, *52* (8), 2322−2331.
(15) Duplantier, A. J.; Kane, C. D.; Bavari, S. Searching for Therapeutics Against Botulinum Neurotoxins: A True Challenge for Drug Discovery. *Curr. Top. Med. Chem.* **2016**, *16* (21), 2330−2349.
(16) Pirazzini, M.; Rossetto, O. Challenges in searching for therapeutics against Botulinum Neurotoxins. *Expert Opin. Drug Discovery* **2017**, *12* (5), 497−510.
(17) Capkova, K.; Salzameda, N. T.; Janda, K. D. Investigations into small molecule non-peptidic inhibitors of the botulinum neurotoxins. *Toxicon* **2009**, *54* (5), 575−82.
(18) Kumar, G.; Swaminathan, S. Recent developments with metalloprotease inhibitor class of drug candidates for botulinum neurotoxins. *Curr. Top. Med. Chem.* **2015**, *15* (7), 685−95.
(19) Burtea, A.; Salzameda, N. T. Discovery and SAR study of a sulfonamide hydroxamic acid inhibitor for the botulinum neurotoxin serotype A light chain. *MedChemComm* **2014**, *5* (6), 706−710.
(20) Thompson, J. C.; Dao, W. T.; Ku, A.; Rodriguez-Beltran, S. L.; Amezcua, M.; Palomino, A. Y.; Lien, T.; Salzameda, N. T. Synthesis and activity of isoleucine sulfonamide derivatives as novel botulinum neurotoxin serotype A light chain inhibitors. *Bioorg. Med. Chem.* **2020**, *28* (18), 115659.
(21) Lai, H.; Feng, M.; Roxas-Duncan, V.; Dakshanamurthy, S.; Smith, L. A.; Yang, D. C. Quinolinol and peptide inhibitors of zinc protease in botulinum neurotoxin A: effects of zinc ion and peptides on inhibition. *Arch. Biochem. Biophys.* **2009**, *491* (1−2), 75−84.
(22) Kumar, G.; Kumaran, D.; Ahmed, S. A.; Swaminathan, S. Peptide inhibitors of botulinum neurotoxin serotype A: design, inhibition, cocrystal structures, structure-activity relationship and pharmacophore modeling. *Acta Crystallogr., Sect. D: Biol. Crystallogr.* **2012**, *68* (5), 511−520.
(23) Kumaran, D.; Adler, M.; Levit, M.; Krebs, M.; Sweeney, R.; Swaminathan, S. Interactions of a potent cyclic peptide inhibitor with the light chain of botulinum neurotoxin A: Insights from X-ray crystallography. *Bioorg. Med. Chem.* **2015**, *23* (22), 7264−73.
(24) Silvaggi, N. R.; Wilson, D.; Tzipori, S.; Allen, K. N. Catalytic features of the botulinum neurotoxin A light chain revealed by high resolution structure of an inhibitory peptide complex. *Biochemistry* **2008**, *47* (21), 5736−45.
(25) Muri, E. M. F.; Nieto, M. J.; Sindelar, R. D.; Williamson, J. S. Hydroxamic Acids as Pharmacological Agents. *Curr. Med. Chem.* **2002**, *9* (17), 1631−1653.
(26) Dickerson, T. J.; Smith, G. R.; Pelletier, J. C.; Reitz, A. B. 8-Hydroxyquinoline and hydroxamic acid inhibitors of botulinum

neurotoxin BoNT/A. *Curr. Top. Med. Chem.* **2014**, *14* (18), 2094−102.
(27) Thompson, A. A.; Jiao, G. S.; Kim, S.; Thai, A.; Cregar-Hernandez, L.; Margosiak, S. A.; Johnson, A. T.; Han, G. W.; O'Malley, S.; Stevens, R. C. Structural characterization of three novel hydroxamate-based zinc chelating inhibitors of the Clostridium botulinum serotype A neurotoxin light chain metalloprotease reveals a compact binding site resulting from 60/70 loop flexibility. *Biochemistry* **2011**, *50* (19), 4019−28.
(28) Brodin, B.; Nielsen, C. U.; Steffansen, B.; Frokjaer, S. Transport of peptidomimetic drugs by the intestinal Di/tri-peptide transporter, PepT1. *Pharmacol. Toxicol.* **2002**, *90* (6), 285−96.
(29) Yang, C. Y.; Dantzig, A. H.; Pidgeon, C. Intestinal peptide transport systems and oral drug availability. *Pharm. Res.* **1999**, *16* (9), 1331−43.
(30) Zhu, T.; Chen, X. Z.; Steel, A.; Hediger, M. A.; Smith, D. E. Differential recognition of ACE inhibitors in Xenopus laevis oocytes expressing rat PEPT1 and PEPT2. *Pharm. Res.* **2000**, *17* (5), 526−32.
(31) Tanaka, M.; Dohgu, S.; Komabayashi, G.; Kiyohara, H.; Takata, F.; Kataoka, Y.; Nirasawa, T.; Maebuchi, M.; Matsui, T. Brain-transportable dipeptides across the blood-brain barrier in mice. *Sci. Rep.* **2019**, *9* (1), 5769.
(32) Silvaggi, N. R.; Boldt, G. E.; Hixon, M. S.; Kennedy, J. P.; Tzipori, S.; Janda, K. D.; Allen, K. N. Structures of Clostridium botulinum Neurotoxin Serotype A Light Chain complexed with small-molecule inhibitors highlight active-site flexibility. *Chem. Biol.* **2007**, *14* (5), 533−42.
(33) Di Blasio, B.; Pavone, V.; Lombardi, A.; Pedone, C.; Benedetti, E. Noncoded residues as building blocks in the design of specific secondary structures: Symmetrically disubstituted glycines and β-alanine. *Biopolymers* **1993**, *33* (7), 1037−1049.
(34) Silhar, P.; Silvaggi, N. R.; Pellett, S.; Capkova, K.; Johnson, E. A.; Allen, K. N.; Janda, K. D. Evaluation of adamantane hydroxamates as botulinum neurotoxin inhibitors: synthesis, crystallography, modeling, kinetic and cellular based studies. *Bioorg. Med. Chem.* **2013**, *21* (5), 1344−8.
(35) Sirimulla, S.; Bailey, J. B.; Vegesna, R.; Narayan, M. Halogen interactions in protein-ligand complexes: implications of halogen bonding for rational drug design. *J. Chem. Inf. Model.* **2013**, *53* (11), 2781−91.
(36) Pettersen, E. F.; Goddard, T. D.; Huang, C. C.; Meng, E. C.; Couch, G. S.; Croll, T. I.; Morris, J. H.; Ferrin, T. E. UCSF ChimeraX: Structure visualization for researchers, educators, and developers. *Protein Sci.* **2021**, *30* (1), 70−82.

https://dx.doi.org/10.1021/acsmedchemlett.0c00674
ACS Med. Chem. Lett. 2021, 12, 295−301